



Low-Loading Ni/Co Catalysts on CeO₂ by Sputtering Deposition for Selective Hydrogen Production via ESR

Letícia Forrer Sosa^{1,2*}, Marco Aurélio Suller Garcia^{2,3,4}, Adriano Friedrich Feil⁵, Dario Eberhardt⁵, Santiago José Alejandro Figueroa⁶, João Monnerat Araújo Ribeiro de Almeida^{1,2}, Pedro Nothaft Romano^{2,4,7}

Resumo/Abstract

RESUMO - Catalisadores mono e bimetálicos de Ni/Co suportados em CeO₂ foram preparados por deposição por magnetron sputtering (SD). A abordagem visou obter 1% em massa de metal total. As caracterizações estruturais e texturais (DRX, fisissorção de N₂, STEM-EDS, TPR, quimissorção de H₂) confirmaram que o método resultou em grande dispersão metálica e interações metal-suporte intensas. O comportamento sinérgico entre o Ni e o Co foi investigado na reação de reforma a vapor de etanol a 500°C e pressão atmosférica. Os catalisadores bimetálicos foram preparados pela deposição simultânea dos metais ou pela modificação na sequência de adição do metal. Dentre os catalisadores que continham Co, o catalisador Ni-Co/CeO₂, no qual o Ni foi depositado antes do que o Co, exibiu uma melhor performance catalítica apresentando uma conversão de etanol acima de 85% e uma seletividade a H₂ de 70% ao longo de toda a reação. A atividade e estabilidade aprimoradas foram atribuídas a uma melhor dispersão metálica, maior interação com o suporte de CeO₂ e a formação de sítios ativos bimetálicos resultantes da sequência de deposição otimizada.

Palavras-chave: Reforma a vapor de etanol, produção de hidrogênio, Magnetron Sputtering, resistência ao coque

ABSTRACT - Monometallic and bimetallic Ni/Co catalysts supported on CeO₂ were prepared by magnetron sputtering deposition (SD). The approach aimed to achieve 1 wt.% of total metal content. Structural and textural characterizations (XRD, N₂ physisorption, STEM-EDS, TPR, H₂ chemisorption) confirmed that the method resulted in high metal dispersion and strong metal-support interactions. The synergistic behavior between Ni and Co was investigated in the ethanol steam reforming reaction (ESR) at 500°C and atmospheric pressure. Bimetallic catalysts were prepared either by simultaneous metal deposition or by varying the sequence of metal addition. Among the catalysts containing Co, the Ni-Co/CeO₂ catalyst -where Ni was deposited prior to Co- exhibited the best catalytic performance showing an ethanol conversion above 85% and hydrogen selectivity of 70% throughout the reaction. The enhanced activity and stability are attributed to improved metal dispersion, stronger interaction with the CeO₂ support, and the formation of more active bimetallic sites resulting from the optimized metal deposition sequence.

Keywords: Ethanol Steam Reforming, Hydrogen Production, Magnetron Sputtering, Coke Resistance

Introduction

Hydrogen is widely used for chemical production, refinery hydrotreatment, and recently in automobile manufacturing (1). Steam reforming (SR) is a well-

established and cost-effective process for producing hydrogen. Ethanol is a renewable source derived from conventional biomass fermentation that can produce hydrogen as feedstock (2,3). The great challenge of SR

¹Instituto de Química, Universidade Federal do Rio de Janeiro (UFRJ), Rio de Janeiro 21941-909, RJ, Brazil.

²LIPCAT (Laboratório de Intensificação de Processos e Catálise), Universidade Federal do Rio de Janeiro (UFRJ), Rio de Janeiro 21941-594, RJ, Brazil.

³Department of Chemistry, Federal University of Maranhão, São Luís 65080-805, MA, Brazil.

⁴Nanotechnology Engineering Program, Alberto Luiz Coimbra Institute for Graduate Studies and Research in Engineering, COPPE, Universidade Federal do Rio de Janeiro (UFRJ), Rio de Janeiro 21941-972, RJ, Brazil.

⁵Bluenano Group, Florianópolis, SC, Brazil.

⁶Laboratório Nacional de Luz Síncrotron (LNLS), Centro Nacional de Pesquisa em Energia e Materiais (CNPEM), Campinas, SP. Brazil.

⁷Campus Duque de Caxias, Universidade Federal do Rio de Janeiro (UFRJ), Rio de Janeiro 25245-390, Brazil.

^{*} leticiaforrer@iq.ufrj.br



reaction is catalyst deactivation, mainly associated with coke formation or sintering; larger particles tend to favor coke deposition and even the growth of carbon nanotubes, depending on the metal (4). Low-cost Ni and Co are considered as promising metals for industrial ethanol steam reforming (ESR) process. Studies show that metals with smaller particle sizes are the most likely to suppress coke formation in ESR (5). Conventional catalyst preparation techniques tend to form particles larger than 10 nm. On the other hand, sputtering deposition (SD) is a technique that allows us to obtain catalysts with homogeneous particles highly dispersed on the catalyst surface. In the methodology used in this work, a highly pure source of the desired metal (99.99%) ejects atoms and/or clusters onto a solid target arranged on a support under mechanical agitation. Our previous work demonstrated the advantages of using the SD method over the conventional incipient impregnation technique in the preparation of the 1%Ni/CeO₂ catalyst. The catalyst prepared by SP showed greater metal-support interaction, improved metallic dispersion and enhanced catalytic activity (6). Taking this into account, in this work, the use of CeO2-supported bimetallic Ni/Co catalysts prepared by SD will be investigated for the ESR and compared with monometallic Ni and Co catalysts. The order of deposition of the metals will also be analyzed.

Experimental

Catalyst preparation

In this work, mono- and bimetallic Ni/Co catalysts supported on a cerium(IV) oxide (CeO₂, nanopowder, < 25 nm, Sigma-Aldrich) were prepared by magnetron sputtering deposition to achieve 1.0 wt.% of active phase (1% Ni or Co for the monometallic and 0.5% Ni and 0.5% Co for the bimetallic ones). The CeO₂ support was placed in a vessel over a mechanical resonant agitator installed inside a vacuum chamber to stir during deposition, ensuring better surface coverage (7,8). For the process, 3 g of CeO₂ were placed into an aluminum support connected to the mechanical resonant agitator inside the vacuum chamber. A vibration frequency of 23 Hz was kept constant during the process. Initially, the vacuum chamber was pumped down by 2 x 10⁻⁷ mbar; then, Ar (99.999%) was introduced up to an operating pressure of 4 x 10⁻³ mbar. The deposition was performed using a 50 W-DC power source with a Ni target of 99.99% and/or a Co target of 99.99% and a diameter of 2". The monometallic catalysts were designated Ni/CeO₂ and Co/CeO2, while the metals' deposition order on the bimetallic catalysts was evaluated. For the Ni-Co/CeO2 catalyst, for example, Ni was deposited first, followed by Co. The opposite occurred for the Co-Ni/CeO₂ catalyst,



while both metals were deposited simultaneously in the NiCo/CeO₂ catalyst.

Catalyst characterization

The Ni and Co metal content in the catalysts was obtained by inductively coupled plasma (ICP). The textural properties of the materials were measured by N_2 physisorption at 77 K using Autosorb iQ equipment (Anton-Paar, Graz, Austria). Before the analysis, the samples (0.18 g) were outgassed under vacuum at 300°C for 18 h. The specific surface areas, pore volume, and pore diameter were estimated using the Brunauer-Emmett-Teller (BET) and Barrett-Joyner-Halenda (BJH) methods. X-ray diffraction (XRD) analyses were performed on an AXRD LPD powder X-ray diffractometer (Proto, Michigan, USA) employing Cu K α radiation at 40 kV and 40 mA. The diffractograms were obtained over a 2 θ range of 20-100° at a scan rate of 0.02°/step and a scan time of 1 s/step.

Temperature-programmed reduction (TPR) and H_2 chemisorption analyses were performed using AutoChem II equipment (Micromeritics). Before reduction, 0.2 g of catalyst was treated in Ar (50 mL/min) at 150°C (10°C/min) for 30 min to remove water. After that, the system was cooled down to 50°C, the gas was switched to 10 (v/v) % H_2 /Ar (50 mL/min), and the temperature increased until 500°C (10°C/min). After that, the samples were cooled down to 40°C, and the catalyst's surface was purged with Ar (50 mL/min) for 30 min; then, the gas was switched to 10 (v/v) % H_2 /Ar, and pulses of a known volume were injected until saturation.

Transmission electron microscopy (TEM) images of the fresh catalysts were acquired using a probe-corrected Titan 80-300 (FEI, Hillsboro, USA) transmission electron microscope, operating at 300 kV, equipped with an Oxford Aztec Energy TEM Advanced Microanalysis System for energy dispersive spectroscopy (EDS) analyses. The imaging was performed in scanning TEM (STEM) mode with a high-angle annular dark-field (HAADF) detector. The samples were prepared by dispersing 1.0 mg of each catalyst in 3 mL of isopropyl alcohol, followed by 10 min of sonication in an ultrasonic bath. Subsequently, one drop of the dispersion was deposited onto a 300-mesh lacey carbon copper grid and allowed to dry at room temperature. The coke content on the spent catalysts was determined by thermogravimetric analysis (TGA) in an SDT 650 Discovery series equipment (TA Instruments, New Castle, USA). For this, the samples (30 mg) were heated from 30°C to 1000°C (5°C/min) under air (100 mL/min).

Catalytic evaluation

The catalytic ethanol steam reforming (ESR) was carried out in a quartz fixed-bed tubular reactor at atmospheric



pressure, loaded with 0.2 g of catalyst. Before the reaction, the catalysts were reduced at 500°C (5°C/min) under a mixture of 25 (v/v) % $\rm H_2/N_2$ (100 mL/min). After reduction, the gas flow was switched to pure $\rm N_2$ (50 mL/min), and an ethanol aqueous solution (0.06 mL/min) with an ethanol:water molar ratio of 1:9 was fed into the reactor by a high-performance liquid chromatography pump. The liquid mixture was heated and vaporized at 200°C, and the reaction was performed using a W/F ratio (catalyst mass/mass flow rate of ethanol) of 0.26 $\rm g_{cat}$ h/ $\rm g_{EtOH}$.

The gas products were analyzed by an online Trace 1610 gas chromatograph (Thermo Scientific) equipped with a flame ionization detector (FID) and a thermal conductivity detector (TCD) containing an RT-Q Bond column (30 m x 0.32 mm x 10 μ m) and a HAYESEP Q 80/100 (2 m x 2 mm) and a Molesieve 13X 80/100 (2 m x 1/8-inch, 2 mm) columns, respectively. The liquid fraction was analyzed by a high-performance liquid chromatography (HPLC), model DIONEX UltiMate 3000 from Thermo Scientific, equipped with a refractive index detector (RID), a Micro-Guard Cation H+ guard column (30 x 4.6 mm, BIORAD), and an Aminex HPX-87H column (300 mm x 7.8 mm, BIORAD). The conversion, product distribution, and H₂ production rate (HPR) were determined by the following equations:

$$EtOH\ conversion\ (\%) = \frac{mol_{EtOH}^0 - \ mol_{EtOH}^t}{mol_{EtOH}^0}\ x\ 100$$

$$Product \ distribution \ (\%) = \frac{mol_{EtoH}^t}{\sum_{i=0}^{N} mol_i^t} \ x \ 100$$

$$HPR\left(\frac{\mathrm{L}}{\mathrm{h}}.\,g_{cat}\right) = \frac{mol_{EtOH}^{0}xY_{H2}x9x22.4}{m_{cat}x\%_{metal}}\;x\;100$$

 Mol^0_{EtOH} and mol^t_{EtOH} are the molar flow rate of ethanol in the feed and at any time t, respectively; mol^t_i are the molar flow rate of the product i at any time t. Y_{H2} is the yield of hydrogen.

Results and Discussion

Characterization of the fresh catalysts

The physicochemical characterization confirmed that all catalysts prepared via SD exhibited high metal dispersion and strong metal-support interactions with CeO₂. The BET surface area of the catalysts remained close to that of pure CeO₂ (47-66 m²·g⁻¹) and no significant differences in the N₂ adsorption-desorption isotherms were observed for the catalysts compared to the bare support, probably due to the low metal loading. The isotherms correspond to the Type IV



isotherm according to the IUPAC classification, which is characteristic of mesoporous materials (9). The expected metal contents (1 wt.% for monometallic and 0.5 wt.% each for bimetallic catalysts) were confirmed by ICP. The SD method allowed controlled deposition of the active phase, including evaluation of the deposition sequence (Ni-Co/CeO₂, Co-Ni/CeO₂, and NiCo/CeO₂). Additionally, H₂ chemisorption revealed high metal dispersion and metallic surface area. XRD patterns showed only CeO₂'s cubic fluorite structure at $2\theta = 28.5^{\circ}$, 33.1° , 47.5° , 56.3° (JCPDS 43-1002) with no detectable Ni or Co phases, suggesting the metallic species' high dispersion or low crystallinity.

STEM-HAADF and EDS analyses revealed that the CeO₂ support has well-defined crystalline facets and uniform nanoparticle sizes, which remain stable after metal deposition (Fig.1). Elemental mapping showed that Ni and Co in the catalyst exist mainly as highly dispersed nanoclusters.

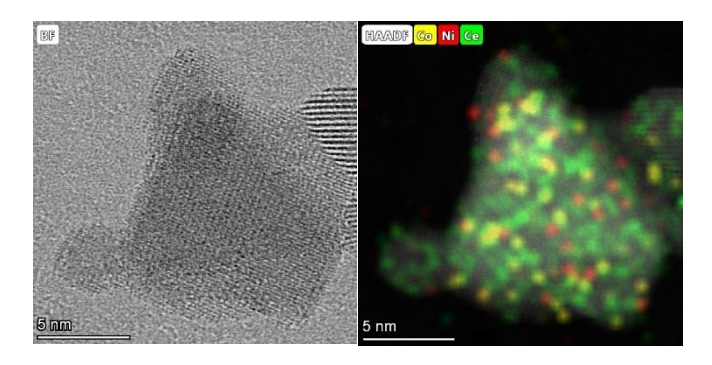


Figure 1. STEM-HAADF (left) and EDS analysis (right) of the NiCo/CeO₂ catalyst.

Catalytic evaluation

In this study, we aimed to improve the performance of the Co-based catalyst (Co/CeO₂), which initially presented high ethanol conversion (~95%) but showed a notable decline over time, reaching approximately 70% after 6 hours of reaction. Although hydrogen production remained relatively stable (~65%), the overall loss in conversion highlighted the need for performance enhancement. To address this, we compared the Co catalyst with a Ni/CeO₂ catalyst (1 wt.% Ni), which demonstrated superior behavior, maintaining conversion above 85% and consistently producing hydrogen at around 70% throughout the first 6 hours. Encouraged by these results, we designed bimetallic systems combining Ni and Co to attempt synergistic improvements.

In the Co-Ni/CeO₂ catalyst, where Co was added prior to Ni (0.5 wt.% each), the performance deteriorated rapidly, with conversion decreasing to ~60% and hydrogen production dropping from ~70% to ~60%. This configuration seemed to hinder catalytic synergy, possibly



due to poor metal dispersion or unfavorable interactions. When both metals were introduced simultaneously (NiCo/CeO₂), the catalyst showed slightly better stability in hydrogen production (~70%), but ethanol conversion remained low (~60-65%), suggesting limited cooperative effects. Finally, when Ni was immobilized first, followed by Co (Ni-Co/CeO₂), the catalyst exhibited significant improvement in the first hours of the reaction showing an ethanol conversion above 90%, however after 6h on-stream its activity matched that of the monometallic Ni/CeO₂ catalyst. The hydrogen production was also very similar to the monometallic Ni catalyst, i.e, 70% throughout the evaluated period. This order of deposition improved the activity of the Ni-Co/CeO₂ catalyst but was not enough to promote its stability.

To better understand the higher initial activity of the Ni-Co/Ceo₂ catalyst, the metal-support interaction effects, metal dispersion and possible alloy formation will be investigated. As well as the causes of deactivation.

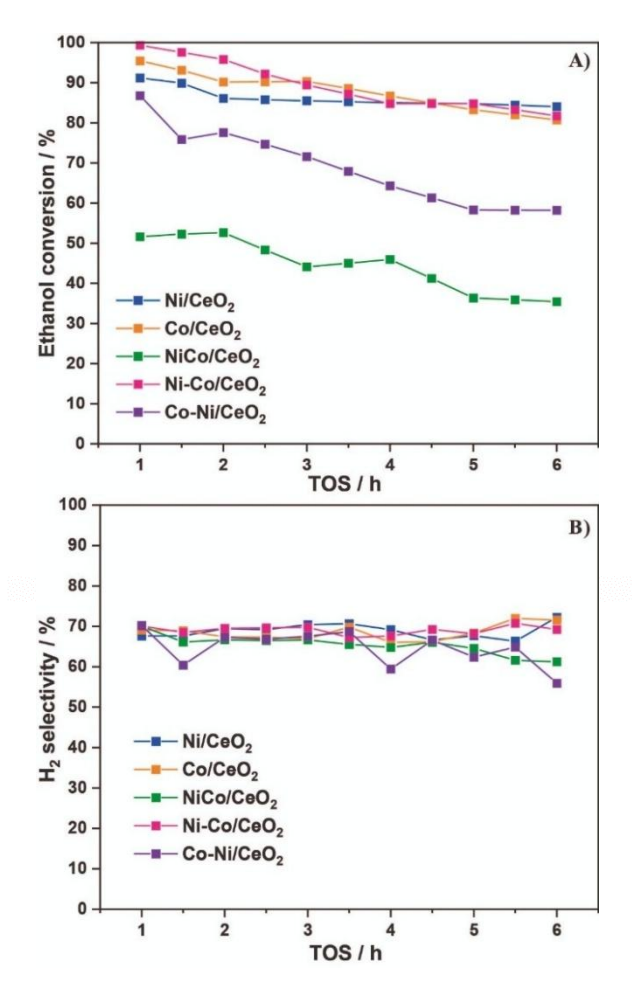


Figure 2. EtOH conversion A) and H_2 selectivity B) for the monoand bimetallic Ni/Co catalysts supported on CeO₂. Reaction conditions: 500° C, S/E = 6, W/F = $0.26~g_{cat}$ h/gEtOH.



Characterization of the spent catalysts

The amount of coke deposited on the spent catalysts was estimated by TPO analyses (**Fig. 3-A**). The coke formation rate in the catalysts occurred in the following order: Co-Ni/CeO₂ (2.1 mg_{coke}/g_{cat} h) > Co/CeO₂ (1.7 mg_{coke}/g_{cat} h) > Ni-Co/CeO₂ (1.4 mg_{coke}/g_{cat} h) > Ni/CeO₂ (1.3 mg_{coke}/g_{cat} h) > NiCo/CeO₂ (1.2 mg_{coke}/g_{cat} h). The results show that the lower stability of Co-containing catalysts is associated with a higher rate of coke formation. Apart from the NiCo/CeO₂ catalyst, which had the lowest coke formation rate, probably due to its low activity, the CeO₂-supported Ni-Co catalyst was the one that most closely resembled the monometallic Ni catalyst in terms of coke formation rate. The addition of 0.5wt.% Ni prevented the high coke formation, even at conversions comparable to the monometallic Co catalyst.

DTG-DSC (**Fig. 3-B**) analyses can be used to evaluate the different types of coke burned in different temperature ranges. Peaks in lower temperatures (< 450°C) are associated with the oxidation of amorphous coke deposited on the surface of metals. On the other hand, peaks at higher temperatures are ascribed to the decomposition of filamentous coke species, which are not close to the metal species (4). Most materials have a peak centered around 300 °C. The Co-Ni/CeO₂ catalyst has two intense peaks at 290 °C and 297 °C. A peak in a higher temperature (592 °C) was observed only for the monometallic Co/CeO₂ catalyst, which suggests that only this catalyst has the contribution of graphitic coke, while in the other catalysts, the metal particles are predominantly encapsulated by amorphous coke.

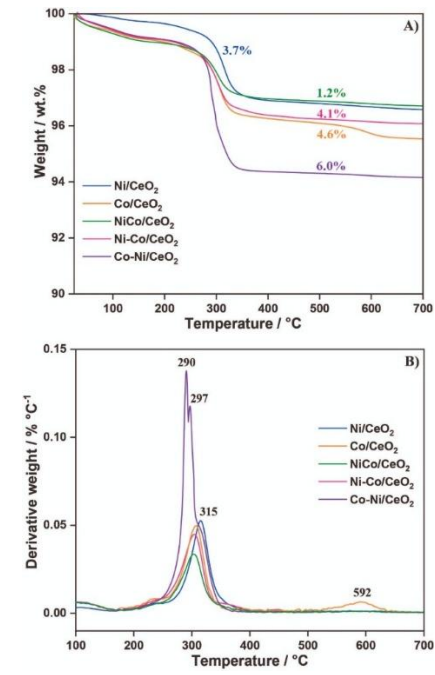


Figure 3. TPO A) and DTG-DSC B) profiles of the spent materials.



Conclusions

This study demonstrates that the catalytic performance and stability of Co-based systems for ethanol steam reforming can be significantly enhanced by the strategic incorporation of Ni and careful control of the metal deposition sequence. While the monometallic Co/CeO₂ catalyst initially exhibited high ethanol conversion, its rapid deactivation over time, attributed to increased coke formation, highlighted the need for improved formulations. In contrast, the Ni/CeO2 catalyst showed superior stability and lower coke accumulation. Among the bimetallic catalysts, the Ni-Co/CeO2 configuration -where Ni was deposited prior to Co- exhibited the best overall performance, but after 6h of reaction reached comparable ethanol conversion (70%) and hydrogen selectivity (70%) to that observed for the monometallic Ni/CeO2 catalyst. TPO and DTG-DSC analyses confirmed that this catalyst, among those containing Co, minimized the formation of both amorphous and graphitic coke species. These findings underscore the critical role of deposition order in optimizing the activity of the catalyst. However, efforts to improve the stability of the Ni-Co/CeO2 catalyst should be made. For this, it's crucial to understand the metal-support interactions, metal dispersion and resistance to deactivation. The magnetron sputtering approach, combined with rational design of bimetallic interfaces, offers a promising route for developing efficient and durable catalysts for hydrogen production via ethanol reforming.

Acknowledgments

We are grateful to the Coordenaçãoo de Aperfeiçoamento de Pessoal de Nível Superior - Brazil (CAPES) and Petrogal Brasil S. A.. This research used facilities of the Brazilian Nanotechnology Laboratory (LNano), part of the Brazilian Center for Research in Energy and Materials (CNPEM), a private non-profit organization under the supervision of the Brazilian Ministry for Science, Technology, and Innovations (MCTI).

References

- 1. Anil, S.; Indraja, S.; Singh, R.; Appari, S.; Roy, B. A. *International Journal of Hydrogen Energy* **2022**, *47*, 8177–8213, doi:10.1016/j.ijhydene.2021.12.183.
- Chen, W.-H.; Biswas, P.P.; Ong, H.C.; Hoang, A.T.; Nguyen, T.-B.; Dong, C.-D. Fuel 2023, 333, 126526, doi:10.1016/j.fuel.2022.126526.
- 3. Deng, Y.; Li, S.; Appels, L.; Zhang, H.; Sweygers, N.; Baeyens, J.; Dewil, R. **2023**, *175*, 113184, doi:10.1016/j.rser.2023.113184.



- 4. Montero, C.; Remiro, A.; Valle, B.; Oar-Arteta, L.; Bilbao, J.; Gayubo, A.G. *Ind. Eng. Chem. Res.* **2019**, *58*, 14736–14751, doi:10.1021/acs.iecr.9b02880.
- 5. Shi, K.; An, X.; Wu, X.; Xie, X. *International Journal of Hydrogen Energy* **2022**, *47*, 39404–39428, doi:10.1016/j.ijhydene.2022.09.097.
- Sosa, L.F.; Garcia, M.A.S.; Silva, A.C.A.; Archanjo, B.S.; Feil, A.F.; Eberhardt, D.; Figueroa, S.J.A.; Almeida, J.M.A.R.D.; Romano, P.N. Applied Catalysis B: Environment and Energy 2025, 365, 124940, doi:10.1016/j.apcatb.2024.124940.
- Languer, M.P.; Scheffer, F.R.; Feil, A.F.; Baptista, D.L.; Migowski, P.; Machado, G.J.; De Moraes, D.P.; Dupont, J.; Teixeira, S.R.; Weibel, D.E. *International Journal of Hydrogen Energy* 2013, 38, 14440–14450, doi:10.1016/j.ijhydene.2013.09.018.
- 8. Gonçalves, R.V.; Vono, L.L.R.; Wojcieszak, R.; Dias, C.S.B.; Wender, H.; Teixeira-Neto, E.; Rossi, L.M. *Applied Catalysis B: Environmental* **2017**, 209, 240–246, doi:10.1016/j.apcatb.2017.02.081.
- 9. Thommes, M.; Kaneko, K.; Neimark, A.V.; Olivier, J.P.; Rodriguez-Reinoso, F.; Rouquerol, J.; Sing, K.S.W. *Pure and Applied Chemistry* **2015**, *87*, 1051–1069, doi:10.1515/pac-2014-1117.